

Potentiometric Determination of Ion-Pair Formation Constants for Cadmium, Calcium Salts, and Cadmium-18-crown-6 Ether Derivative Complexes with a Sulfate Ion in Water

Yoshihiro Kudo,* Sasagu Takeuchi, Yota Kobayashi, Shoichi Katsuta, and Yasuyuki Takeda

Department of Chemistry, Faculty of Science, Chiba University, 263-8522 Chiba, Japan

Theoretical equations were derived for the determination of ion-pair formation constants (K^0 in $\text{mol}^{-1}\cdot\text{dm}^3$) for 2:2 ($\text{M}^{2+}\text{X}^{2-}$) and 2:1 electrolytes and MX with crown ethers (L) in water at an ionic strength of zero. The K^0 values were determined potentiometrically at 25 °C; CdSO_4 , CdCl_2 , $\text{Cd}(\text{picrate})_2$, CaCl_2 , and $\text{Ca}(\text{picrate})_2$ were used as the electrolytes, and $\text{CdL}^{2+}\text{SO}_4^{2-}$ with L = 18-crown-6 ether (18C6) and benzo-18C6 were used as the ion-pair complexes. By examining the validity of the equations directly or indirectly, the K^0 values for CdSO_4 and CdCl_2 were compared with the corresponding literature. Consequently, it was evident that the derived equations are useful for the determination of K^0 .

Introduction

It has been known that univalent metal complex ions with crown ether (L) form some ion-pairs in water in association with several anions (X^-), such as picrate (Pic^-), perchlorate, and permanganate ions.^{1,2} With this process taken into account, extraction of univalent metal ions by L into many organic solvents has been analyzed exactly from a chemical equilibrium point of view,^{3,4} and thereby detailed characteristics of such extraction systems have been clarified.^{1,3} However, the same analysis for the extraction equilibria of divalent metal salts (MX_z , $z = 1$ or 2) with L as that for those of the univalent metal salts seems to have not been studied so far. The reason the analysis has not been performed may be due to the lower stabilities in water of the divalent metal complex ions, ML^{2+} , compared with M(II) chelate compounds.

In the process of such extraction studies of MX_z with L, we derive in the present paper theoretical equations for the potentiometric determination of ion-pair formation constants (K_{MX}^0 for $z = 1$ and K_1^0 or K_2^0 for $z = 2$) of MX_z and those (K_{MLX}^0) of its 1:1 : 1 ion-pair complexes at an ionic strength (I) of zero and then try to determine their K^0 values at 25 °C in water. Therefore, the ion-pair (or complex) formation of CdSO_4 , CdCl^+ , CdCl_2 , CdPic^+ , CaCl^+ , and CaPic^+ , $\text{Cd}(\text{18C6})\text{SO}_4$, and $\text{Cd}(\text{B18C6})\text{SO}_4$ was examined, where 18C6 and B18C6 denote 18-crown-6 ether and its monobenzo derivative, respectively. Especially, the two cations with Pic^- will be important for solvent extraction studies in the future. For the CdSO_4 and CdCl_2 systems, the K^0 values determined here were compared with those^{5–7} reported previously, and the values were in good agreement.

Experimental Section

Chemicals. Cadmium picrate was prepared by adding an aqueous solution of suspended $\text{Ba}(\text{OH})_2$ (guaranteed reagent, Wako, Osaka, Japan) into a mixture at a molar ratio of 1 to 2 of $\text{CdSO}_4 \cdot \{8/3\}\text{hydrate}$, 99.0 % grade, Kanto, Tokyo, Japan} with HPic (guaranteed reagent, Wako). The barium sulfate precipitate was filtered, and the filtrate was concentrated with

an evaporator (type RE1-N, Iwaki Glass Co. Ltd., Chiba, Japan) and then was allowed to stand for several hours. The yellow needle crystals deposited were filtered and dried in vacuo for 20 h. The amounts of Cd^{2+} , Pic^- , and water involved in the crystal were analyzed by a chelatometric titration with EDTA, spectrophotometric measurements at 356 nm, and a Karl Fischer titration, respectively. Anal.: $\text{Cd}(\text{Pic})_{2.2}\cdot 4.5\text{H}_2\text{O}$. Calcium picrate was prepared by mixing a suspended solution of $\text{Ca}(\text{OH})_2$ (<96.0 % grade, Kanto) with an aqueous solution of HPic at a molar ratio of 1 to 2. This mixture was concentrated as described above, and the yellow needles were crystallized from its concentrated mixture. Then, the yellow crystals were filtered and dried in vacuo at room temperature. The analysis was performed according to the same method as that described for $\text{Cd}(\text{Pic})_2$. Anal.: $\text{Ca}(\text{Pic})_{2.1}\cdot 4.1\text{H}_2\text{O}$ (dried for 58 h) or $\text{Ca}(\text{Pic})_{2.0}\cdot 4.6\text{H}_2\text{O}$ (dried for 22 h). The purities of $\text{Cd}(\text{NO}_3)_2\cdot 4\text{H}_2\text{O}$ (98 % grade, Kanto), $\text{CdCl}_2\cdot (5/2)\text{H}_2\text{O}$ (99 % grade, Kanto), $\text{CdSO}_4\cdot (8/3)\text{H}_2\text{O}$ (see above), $\text{Ca}(\text{NO}_3)_2\cdot \text{H}_2\text{O}$ (guaranteed reagent, Kanto), and $\text{CaCl}_2\cdot 2\text{H}_2\text{O}$ (guaranteed reagent, Kanto) were checked by the chelatometric titration and then employed for emf measurements (see below). 18-Crown-6 ether and B18C6 were purified according to the method described previously.⁸ Other chemicals were of analytical grade and used without further purification. Water was distilled once and was purified by passage through a Milli-Q Lab system (Millipore).

Emf Measurements. The electrochemical cells used for the present emf measurements were as follows: $\text{Ag}|\text{AgCl}|0.1\text{ mol}\cdot\text{dm}^{-3}(\text{C}_2\text{H}_5)_4\text{NCl}|\text{test solution}|\text{M}^{2+}\text{-selective electrode (cell I)}^9$ and $\text{Ag}|\text{AgCl}|0.1\text{ mol}\cdot\text{dm}^{-3}\text{ KCl or }(\text{C}_2\text{H}_5)_4\text{NCl}|1\text{ mol}\cdot\text{dm}^{-3}\text{ MNO}_3(\text{M} = \text{Na and K})|\text{test solution}|\text{M}^{2+}\text{-selective electrode (cell IM)}$. As the test solutions, aqueous solutions of $\text{Cd}(\text{NO}_3)_2$ or $\text{Ca}(\text{NO}_3)_2$ were used for the preparation of calibration curves, those of CdSO_4 , CdCl_2 , $\text{Cd}(\text{Pic})_2$, CaCl_2 , or $\text{Ca}(\text{Pic})_2$ for the determination of K_{MX} or K_1 and K_2 , and those of CdSO_4 with 18C6 and B18C6 for the determination of K_{MLX} . Cadmium chloride was measured by using the cell IK, because the reasonable K values were not available from the measurements with the cell I. The emf values of the CdSO_4 system were also measured with the cell IK. The cells I and IK were used in the

* Corresponding author. E-mail: iakudo@faculty.chiba-u.jp.

Table 1. Ion-Pair Formation Constants,^a K_1^0 and K_2^0 , of MX_2 in Water at $T = 298 \text{ K}$

MX_2	K_1^0		K_2^0	
	$\text{mol}^{-1}\cdot\text{dm}^3$		$\text{mol}^{-1}\cdot\text{dm}^3$	
CdCl_2	$86 \pm 30,^b$	$89 \pm 15,^{b,c}$	$100,^d$	$8.7 \pm 7.5,^{b,c}$
	$91,^e$		$25,^f$	$38.5,^g$
$\text{Cd}(\text{Pic})_2$	$108 \pm 11, 107 \pm 17^h$		<i>i</i>	
CaCl_2	40 ± 7		<i>i</i>	
$\text{Ca}(\text{Pic})_2$	88 ± 58		<i>i</i>	

^a Average value \pm its standard deviation or standard error determined at $I = 0 \text{ mol}\cdot\text{dm}^{-3}$. ^b Values determined by the cell IK. ^c Values based on the DeFord–Hume method or the method by Vanderzee and Dawson. ^d Reference 5. ^e Value estimated from the $K_1^0(m)$ value ($= 1/0.011 \text{ mol}^{-1}\cdot\text{kg}$) at dilute solution in the molality unit with $K_1^0 = K_1^0(m)/0.9970480$. See ref 6. ^f Values determined by solubility measurement at $I = 3.00 \text{ mol}\cdot\text{dm}^{-3}$ (NaClO_4). See ref 17. ^g Values determined by calorimetric titration at $I = 3.00 \text{ mol}\cdot\text{dm}^{-3}$ (NaClO_4). See ref 18. ^h Values determined by adding the data for the cell INa $\{bs = (1.6 \pm 0.1) \cdot 10^{-3} \text{ mol}\cdot\text{dm}^{-3}$, $R = 0.981$, and $n = 55\}$ to that for I. ⁱ Not determined.

K_{MLX} determination. A molar ratio of $[\text{L}]/[\text{CdSO}_4]_t$ was fixed at unity,⁹ because of the major formation of CdL^{2+} complex: $[\]_t$ indicates a total concentration of L or MX_2 .

The emf values were measured at $25 \pm 0.4 \text{ }^\circ\text{C}$ with a Horiba pH/ion meter F-23 equipped with Horiba ion-selective electrodes, type 8007-10C for Cd^{2+} and type 8203-10C for Ca^{2+} , and Horiba reference electrodes, types 2660A-10T and 2565A-10T (a double-junction type, for the cell IM). A deterioration of the Ca^{2+} -selective electrode was observed with coloring of its liquid membrane in the emf measurements of the $\text{Ca}(\text{Pic})_2$ solutions, and then the electrode exhibited a non-Nernstian response with slopes of less than 20 mV/decade. The larger deviation of the K_1^0 value for the $\text{Ca}(\text{Pic})_2$ system may come from such an instability of the electrode, compared with the other systems (see Table 1).

Calculation of the Ion-Pair Formation Constants. The emf values of the calibration curves, emf versus $\log[\text{Cd}(\text{NO}_3)_2]_t$ or $\log[\text{Ca}(\text{NO}_3)_2]_t$, for the cells I and INa were corrected by estimating liquid junction potentials (E_{LJ}) with the Henderson equation.⁹ In the determination of experimental equilibrium constants ($K_{\text{MX}}^{\text{exptl}}$ and K_1^{exptl} , see Theory for definition) for MX and MX_2 , E_{LJ} was treated with a function of $[\text{M}^{2+}]$, which shows a molar concentration of a free metal ion M^{2+} in water. Here, the value of $2 \times$ (the slope of the calibration curve) was employed as the $2.3RT/F$ term on the Henderson equation. First, $\log[\text{M}^{2+}]$ was calculated from an equation of $\log[\text{M}^{2+}] = \{\text{emf} - E_{\text{LJ}} - (\text{intercept of the calibration curve})\}/(\text{slope of the calibration curve})$. Next, this $[\text{M}^{2+}]$ value was introduced into E_{LJ} and then the second E_{LJ} value was obtained. Furthermore, this value was introduced into the equation of $\log[\text{M}^{2+}]$. These calculations were repeated successively until $[\text{M}^{2+}]$ became invariable.⁹ Then, the $K_{\text{MX}}^{\text{exptl}}$ or K_1^{exptl} values were computed by using the $[\text{M}^{2+}]$ thus obtained. The same is essentially true for the $K_{\text{MLX}}^{\text{exptl}}$ calculation (see Theory for this symbol). On the other hand, $\log[\text{M}^{2+}]$ for the cell IK was simply calculated from the equation of $\log[\text{M}^{2+}]$ without E_{LJ} .

In the calculation of E_{LJ} , mobilities of CaPic^+ , CaCl^+ , CdPic^+ , and CdL^{2+} at infinite dilution were assumed from their sizes and so on to be equal to those of Pic^- , Ca^{2+} , Pic^- , and Cd^{2+} , respectively, because their data could not be found. There were little differences in molar conductivity between CdL^{2+} at $[\text{L}]/[\text{Cd}^{2+}]_t \approx 1$ and free Cd^{2+} .^{10,11}

Ion size parameters used for the calculation of $\log y_{2+}$, $\log y_+$, $\log y_{2-}$, or $\log y_-$ (see Theory for these symbols) were 5 \AA

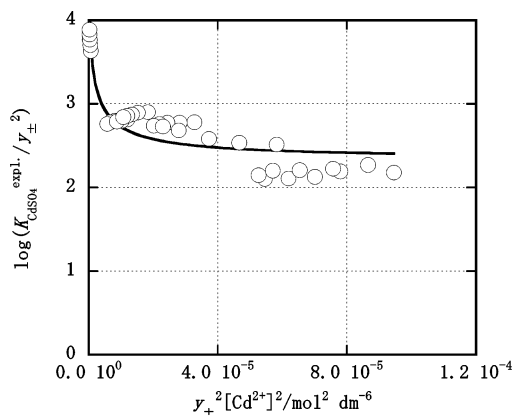


Figure 1. Plot of $\log(K_{\text{CdSO}_4}^{\text{exptl}}/y_{\pm}^2)$ versus $y_{\pm}^2[\text{Cd}^{2+}]^2$. Solid line shows the curve fitted to eq 1 by the nonlinear regression.

for Cd^{2+} , 6 \AA for Ca^{2+} , 4 \AA for CdCl^+ and SO_4^{2-} , 3 \AA for Cl^- , and 7 \AA for Pic^- .¹² The parameter of CaCl^+ that has a composition similar to that of CdCl^+ was approximated to be 4 \AA , because its parameter was not available. Also, it was assumed that the parameters of CdPic^+ and CaPic^+ were equal to that of Pic^- .

Complex formation constants (K_{ML} , see Theory) used for the calculation of $K_{\text{MLX}}^{\text{exptl}}$ were as follows: $10^{-0.053} \text{ mol}^{-1}\cdot\text{dm}^3$ for $\text{Cd}(\text{18C6})^{2+}$ and $10^{0.11}$ for $\text{Cd}(\text{B18C6})^{2+}$ in water at $25 \text{ }^\circ\text{C}$.^{10,11} These values were treated as constants being independent of I in the calculation.⁹

Theory

2:2 Electrolytes. The following equilibrium is proposed for the derivation of an analytical equation: $\text{M}^{2+} + \text{X}^{2-} \rightleftharpoons \text{MX}$. Here, its concentration equilibrium constant, K_{MX} , is defined as $[\text{MX}]/[\text{M}^{2+}][\text{X}^{2-}]$. Mass and charge balance equations are expressed as $[\text{MX}]_t = [\text{M}^{2+}] + [\text{MX}] + bs = [\text{X}^{2-}] + [\text{MX}] + bs$ and $[\text{M}^{2+}] = [\text{X}^{2-}]$; a parameter (bs) is assumed to be constant and indicates an amount of species s ($= \text{MX}$) lost from the bulk of the test solution, as described previously.⁹ The experimental equilibrium constant, $K_{\text{MX}}^{\text{exptl}}$, is obtained from $K_{\text{MX}}^{\text{exptl}} = ([\text{MX}]_t - [\text{M}^{2+}])/[\text{M}^{2+}]^2$; the molar concentration $[\text{M}^{2+}]$ has been determined potentiometrically.⁹ From these equations, the following one is derived: $K_{\text{MX}}^{\text{exptl}}/y_{\pm}^2 - (bs/y_{\pm}^2[\text{M}^{2+}]^2) = K_{\text{MX}}^0$. Here, y_{\pm} and K_{MX}^0 denote a mean ionic activity coefficient estimated from the extended Debye–Hückel law (EDHL) and a thermodynamic equilibrium constant (or that at $I = 0 \text{ mol}\cdot\text{dm}^{-3}$), respectively; an activity coefficient (y_0) of the neutral species MX (and MLX) is approximated to be unity.⁹ Rearranging the equation and taking logarithms of both sides in it, a final form is obtained as

$$\log \left(\frac{K_{\text{MX}}^{\text{exptl}}}{y_{\pm}^2} \right) = \log \left(K_{\text{MX}}^0 + \frac{bs}{y_{\pm}^2[\text{M}^{2+}]^2} \right) \quad (1)$$

Hence, as described before,¹³ the two parameters, K_{MX}^0 and bs , are yielded by a nonlinear regression analysis⁹ from $\log(K_{\text{MX}}^{\text{exptl}}/y_{\pm}^2)$ plotted against $y_{\pm}^2[\text{M}^{2+}]^2$ (see Figure 1). Equation 1 shows that the higher $[\text{M}^{2+}]$ is, the less effective bs becomes.⁹

2:1 Electrolytes. For this case, the following equilibria are proposed: $\text{M}^{2+} + \text{X}^- \rightleftharpoons \text{MX}^+$ and $\text{MX}^+ + \text{X}^- \rightleftharpoons \text{MX}_2$. Similarly, these mass and charge balance equations are

$$[\text{MX}_2]_t = [\text{M}^{2+}] + [\text{MX}^+] + [\text{MX}_2] \quad (\text{for } \text{M}^{2+}) \quad (2)$$

$$2[\text{MX}_2]_t = [\text{X}^-] + [\text{MX}^+] + 2[\text{MX}_2] \quad (\text{for } \text{X}^-) \quad (2a)$$

and

$$2[\text{M}^{2+}] + [\text{MX}^+] = [\text{X}^-] \quad (3)$$

Also, the concentration equilibrium constants are defined as

$$K_1 = [\text{MX}^+]/[\text{M}^{2+}][\text{X}^-] \quad (4)$$

and

$$K_2 = [\text{MX}_2]/[\text{MX}^+][\text{X}^-] \quad (5)$$

On the basis of the previous paper,⁶ we assumed here that $[\text{M}^{2+}] + [\text{MX}^+] \gg [\text{MX}_2]$ and $([\text{X}^-] + [\text{MX}^+])/2 \gg [\text{MX}_2]$. This means $K_2 \approx 0$; that is, the second-step association of MX^+ with X^- is negligible. Two cases for dependence of $\log K_1$ on I were observed in the present experiments. For case A, the I dependence of $\log K_1$ is like a hyperbola,⁹ and for case B, $\log K_1$ is apparently independent of I .

Case (A): From eqs 2 and 3, mass and charge balance equations with bs are expressed as $[\text{MX}_2]_t = [\text{M}^{2+}] + [\text{MX}^+] + bs = ([\text{X}^-] + [\text{MX}^+] + bs)/2$ and $2[\text{M}^{2+}] + [\text{MX}^+] + bs = [\text{X}^-]$. Here, the parameter bs indicates an amount of MX^+ (= s) lost from the test solution.⁹ From these equations and eq 4, we can easily derive the equation

$$K_1 = \frac{[\text{MX}_2]_t - [\text{M}^{2+}] - bs}{[\text{M}^{2+}][\text{X}^-]} = K_1^{\text{exptl}} - \frac{bs}{[\text{M}^{2+}][\text{X}^-]} \quad (6)$$

with $[\text{X}^-] = [\text{MX}_2]_t + [\text{M}^{2+}]$ and $K_1^{\text{exptl}} \equiv ([\text{MX}_2]_t - [\text{M}^{2+}])/[\text{M}^{2+}][\text{X}^-]$. Transforming K_1 into a thermodynamic K_1 (K_1^0) with the activity coefficients, rearranging it, and then taking logarithms of the both sides, the following equation is obtained:

$$\log \left(\frac{y_+ K_1^{\text{exptl}}}{y_{2+} y_-} \right) = \log \left(K_1^0 + \frac{y_+ bs}{y_{2+} y_- [\text{M}^{2+}][\text{X}^-]} \right) \quad (6a)$$

y_+ , y_{2+} , and y_- denote the activity coefficients of MX^+ , M^{2+} , and X^- in water, respectively (see Experimental Section). Similar to eq 1, eq 6a is applicable to nonlinear regression analysis. Their terms, $\log(y_+ K_1^{\text{exptl}}/y_{2+} y_-)$ and $y_{2+} y_- [\text{M}^{2+}][\text{X}^-]/y_+$, correspond to $\log(K_{\text{MX}}^{\text{exptl}}/y_{\pm}^2)$ and $y_{\pm}^2 [\text{M}^{2+}]^2$ in eq 1, respectively.

Case (B): The K_1^0 value is obtained from an average. Namely, it is calculated from the $y_{\pm} K_1^{\text{exptl}}/y_{2+} y_-$ term in eq 6a.

2:2 Electrolytes in Complexation with L. As reported previously for 1:1 electrolyte systems with L,⁹ we assumed three equilibria as follows: $\text{M}^{2+} + \text{X}^{2-} \rightleftharpoons \text{MX}$, $\text{M}^{2+} + \text{L} \rightleftharpoons \text{ML}^{2+}$, and $\text{ML}^{2+} + \text{X}^{2-} \rightleftharpoons \text{MLX}$. The concentration equilibrium constants corresponding to the latter two are defined as $K_{\text{ML}} = [\text{ML}^{2+}]/[\text{M}^{2+}][\text{L}]$ (see Experimental Section) and $K_{\text{MLX}} = [\text{MLX}]/[\text{ML}^{2+}][\text{X}^{2-}]$, respectively. Mass and charge balance equations are

$$[\text{MX}]_t = [\text{M}^{2+}] + [\text{MX}] + [\text{ML}^{2+}] + [\text{MLX}] + bm \quad (\text{for } \text{M}^{2+}) \quad (7)$$

$$= [\text{X}^{2-}] + [\text{MX}] + [\text{MLX}] + bm \quad (\text{for } \text{X}^{2-}) \quad (7a)$$

$$[\text{L}]_t = [\text{L}] + [\text{ML}^{2+}] + [\text{MLX}] + bm' \quad (8)$$

and

$$[\text{M}^{2+}] + [\text{ML}^{2+}] = [\text{X}^{2-}] \quad (9)$$

Solving these equations for $[\text{X}^{2-}]$, we can obtain

$$[\text{X}^{2-}] = \frac{[\text{M}^{2+}]\{1 + K_{\text{ML}}([\text{M}^{2+}] + [\text{L}]_t - [\text{MX}]_t + bm - bm')\}}{1 - K_{\text{ML}}K_{\text{MX}}[\text{M}^{2+}]^2} \quad (10)$$

Also, under the condition of $[\text{MX}]_t = [\text{L}]_t$ and for the hypothesis of $bm \approx bm'$, that is, $1 + K_{\text{ML}}[\text{M}^{2+}] \gg K_{\text{ML}}(bm - bm')$, this equation becomes

$$[\text{X}^{2-}] = \frac{[\text{M}^{2+}](1 + K_{\text{ML}}[\text{M}^{2+}])}{1 - K_{\text{ML}}K_{\text{MX}}[\text{M}^{2+}]^2} \quad (10a)$$

Equation 9 gives

$$[\text{ML}^{2+}] = [\text{X}^{2-}] - [\text{M}^{2+}] \quad (11)$$

and then a combination of eq 7a and K_{MX} (see 2:2 Electrolytes) yields

$$[\text{MLX}] = [\text{MX}]_t - [\text{X}^{2-}]\beta - bm \quad (12)$$

with $\beta = 1 + K_{\text{MX}}[\text{M}^{2+}]$. From the thermodynamic definition of K_{MLX} combined with eqs 10a, 11, and 12, therefore, we can derive the following equation:

$$K_{\text{MLX}}^0 = \frac{[\text{MX}]_t - [\text{X}^{2-}]\beta - bm}{y_{\pm}^2 [\text{ML}^{2+}][\text{X}^{2-}]} \quad (\text{here } y_0 \approx 1) \quad (13)$$

Rearranging this equation and then taking logarithms of both sides, the equation

$$\log \left(\frac{K_{\text{MLX}}^{\text{exptl}}}{y_{\pm}^2} \right) = \log \left(K_{\text{MLX}}^0 + \frac{bm}{y_{\pm}^2 [\text{ML}^{2+}][\text{X}^{2-}]} \right) \quad (13a)$$

is obtained with $K_{\text{MLX}}^{\text{exptl}} = ([\text{MX}]_t - [\text{X}^{2-}]\beta)/([\text{X}^{2-}] - [\text{M}^{2+}][\text{X}^{2-}]$. Equation 13a makes the same analysis as that for eq 1 possible to us, when $\log(K_{\text{MLX}}^{\text{exptl}}/y_{\pm}^2)$ was plotted against $y_{\pm}^2 [\text{ML}^{2+}][\text{X}^{2-}]$.

Results and Discussion

Ion-Pair Formation of CdSO_4 . Figure 1 shows a plot of $\log(K_{\text{CdSO}_4}^{\text{exptl}}/y_{\pm}^2)$ versus $y_{\pm}^2 [\text{Cd}^{2+}]^2$ based on eq 1, where y_{\pm}^2 is defined as $y_{2+} y_{2-}$ and y_{2+} and y_{2-} denote ionic activity coefficients of M^{2+} and SO_4^{2-} in water, respectively. The plot was similar to those reported for the 1:1 electrolyte systems such as NaPic , NaMnO_4 , and NaReO_4 . The nonlinear regression analysis of the plot by eq 1 gave $K_{\text{CdSO}_4}^0 = 221 \pm 31 \text{ mol}^{-1} \cdot \text{dm}^3$ and $bs = (3.1 \pm 0.6) \cdot 10^{-3} \text{ mol} \cdot \text{dm}^{-3}$ with a fitting curve of R (correlation coefficient) = 0.907 at n (number of data) = 41. This $K_{\text{CdSO}_4}^0$ value is in agreement with those (212 and $1/0.0051 \text{ mol}^{-1} \cdot \text{dm}^3$) reported by conductometry⁷ and the excess chemical potential method.¹⁴ This indicates that the present procedure is essentially reasonable, as that reported previously for the 1:1 electrolyte systems.⁹ The $K_{\text{CdSO}_4}^0$ value is much larger than that ($0.15 \text{ mol}^{-1} \cdot \text{dm}^3$ at 25°C and $I = 0$) for a contact ion-pair formation estimated from Raman and IR spectroscopic data.¹⁵ This finding may mean that the $K_{\text{CdSO}_4}^0$ value determined here is of a mixture of the contact ion-pair (or the inner-sphere complex) with outer-sphere and outer-outer-sphere complexes.^{15,16}

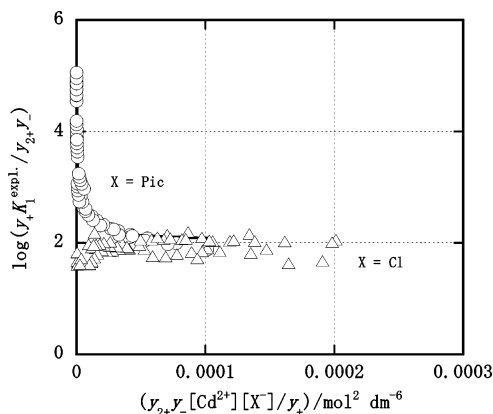


Figure 2. Plots of $\log(y_+K_1^{\text{exptl}}/y_{2+y_-})$ versus $y_{2+y_-}[\text{Cd}^{2+}][\text{X}^-]/y_+$ for X = Pic (circle) and Cl (triangle). Solid line for the Cd(Pic)₂ system shows the curve fitted to eq 6a by the regression.

Ion-Pair Formation of 2:1 Electrolytes. Figure 2 shows plots of $\log(y_+K_1^{\text{exptl}}/y_{2+y_-})$ versus $y_{2+y_-}[\text{Cd}^{2+}][\text{Pic}^-]/y_+$ and $y_{2+y_-}[\text{Cd}^{2+}][\text{Cl}^-]/y_+$. The plot for Cd(Pic)₂ gave a hyperbolic curve, so this system is classified as case A (see Theory). Equation 6a reproduced well the plot related to $\log K_1^{\text{exptl}}$ in terms of the regression analysis (the curve of X = Pic in Figure 2). Thereby, $K_1^0 = 108 \pm 11 \text{ mol}^{-1}\cdot\text{dm}^3$ and $bs = (1.3 \pm 0.1) \cdot 10^{-3} \text{ mol}\cdot\text{dm}^{-3}$ with a curve of $R = 0.945$ were obtained at $n = 30$. Similar results were given for the CaCl₂ $\{bs = (6.9 \pm 0.6) \cdot 10^{-4}, R = 0.964$ and $n = 65\}$ and Ca(Pic)₂ $\{bs = (8.1 \pm 1.1) \cdot 10^{-4}, R = 0.969$ and $n = 27\}$ systems. On the other hand, the CdCl₂ system differed from these three systems. This plot is independent of the $y_{2+y_-}[\text{Cd}^{2+}][\text{Cl}^-]/y_+$ axis (the triangle in Figure 2). This system corresponds to case B. Hence, we can simply obtain $K_1^0 = 86 \pm 30 \text{ mol}^{-1}\cdot\text{dm}^3$ ($n = 65$) on the average from the $y_+K_1^{\text{exptl}}/y_{2+y_-}$ values. These K_1^0 values are listed in Table 1, together with those reported before.^{5,6,17,18} The K_1^0 value for CdCl⁺ is in agreement with the values reported before within experimental error. Hence, it is not clear where the difference between the two cases, A and B, comes from.

Furthermore, a modification of the DeFord–Hume method^{19,20} or the method by Vanderzee and Dawson⁵ was applied for an analysis of the CdCl₂ system. From eqs 2, 4, and 5, the following relationship is obtained:

$$[\text{MX}_2]_t/[\text{M}^{2+}] = 1 + K_1[\text{X}^-] + K_1K_2[\text{X}^-]^2 \quad (2b)$$

Then, replacing $[\text{MX}_2]_t$, $[\text{M}^{2+}]$, and $[\text{X}^-]$ by a_t , a_M , and a_X and assuming $a_t = \sqrt[3]{y_{2+y_-} \cdot \sqrt[3]{4} [\text{MX}_2]_t}$,²¹ we have

$$a_t/a_M = 1 + K_1^0 a_X + K_1^0 K_2^0 (a_X)^2 \quad (2c)$$

with $a_M = y_{2+}[\text{M}^{2+}]$, $a_X = y_-[\text{X}^-]$, and $K_2^0 \equiv y_0[\text{MX}_2]/y_{+-}[\text{MX}^+]a_X$. Here, a_t , a_M , and a_X denote a mean activity for the 2:1 electrolyte MX₂ in water,²¹ an ionic activity of M²⁺, and that of X⁻, respectively. This equation shows, when a_t/a_M is assumed to be a function of the ionic activity a_X , the values that K_1^0 and K_2^0 can take. Also, one can see that eq 2c becomes a polynomial equation for a_X and then a_t/a_M corresponds to the DeFord–Hume function²⁰ expressed as $F_0(X)$ or the function f^0 described by Vanderzee and Dawson.⁵ When a_t/a_M is plotted against a_X , we can obtain the K_1^0 and K_2^0 values from the nonlinear regression analysis. Figure 3 shows the plot of a_t/a_M against a_X . From this plot, we had an experimental equation: $a_t/a_M = (1.548 \pm 0.041) + (138 \pm 23)a_X + (138 \pm 23)(8.66 \pm$

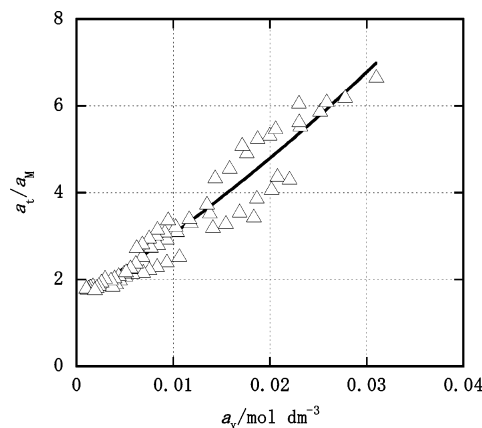


Figure 3. Plot of a_t/a_M versus a_X for the CdCl₂ system. Solid line shows the curve fitted to eq 2c by the regression.

$7.48)(a_X)^2$ at $R = 0.959$ and $n = 67$. Correcting a deviation of the intercept, 1.548, from unity,²¹ then K_1^0 and K_2^0 were estimated to be $89 \pm 15 \{ = (138/1.548) \pm |89| \cdot \sqrt{(23/138)^2 + (0.041/1.548)^2} \}$ and $8.7 \pm 7.5 \text{ mol}^{-1}\cdot\text{dm}^3$, respectively. Thus, the estimated K_1^0 value is in good agreement with that determined by eq 6a. Also, in addition to this, the K_2^0 value is equal to that reported by Vanderzee and Dawson⁵ within experimental error. From these facts, the essential validity of eq 2c is demonstrated for the analysis of K_1^0 at least. Table 1 lists the K_1^0 and K_2^0 values thus determined for the CdCl₂ system.

From eqs 4 and 5, K_1^0 and K_2^0 , we have the relationships of $y_+K_1/y_{2+y_-} = K_1^0$ and $y_0K_2/y_{+-} = K_2^0$. Therefore, the following equation is obtained: $K_1K_2/K_1^0K_2^0 = y_{2+}(y_-)^2$. From this equation and the K values at $I = 3 \text{ mol}\cdot\text{dm}^{-3}$ of the CdCl₂ system listed in Table 1, the mean ionic activity coefficient γ_{\pm} for the CdCl₂ solution with a large excess of NaClO₄ (and NaCl and HClO₄¹⁷ or NaCl¹⁸ as minor electrolytes) can be estimated to be 0.58 or 0.60 ($= \sqrt[3]{y_{2+}(y_-)^2} = \sqrt[3]{K_1K_2/K_1^0K_2^0}$). Although there is a difference in a concentration unit, these values are close to an activity coefficient, 0.611 (see Table 10 in Appendix 8–10 in ref 21), reported before for a 3.0 mol·kg⁻¹ NaClO₄ solution. The same coefficient estimated from the other K values in Table 1 is also 0.683: $K_1K_2 = 160 \text{ mol}^{-2}\cdot\text{dm}^6$ at 25 °C and $I = 3.0 \text{ mol}\cdot\text{dm}^{-3}$ (NaClO₄ solution with HClO₄ and NaCl as minor electrolytes).⁵ These results indicate that eq 2c is useful for determining K_1^0 and K_2^0 . In addition to this, the fact that the y_{\pm} value for the CdCl₂ solution is practically dependent on I due to “NaClO₄ added to excess” into the solution is consistent with that known generally.

The K_1^0 value for the CdCl₂ system is larger than the corresponding value of K_2^0 (Table 1). This is consistent with a tendency for the complex formation of Cd²⁺ with F⁻, Cl⁻, Br⁻, and I⁻ in water ($I = 1 \text{ mol}\cdot\text{dm}^{-3}$ for F⁻, $I = 3$ for others,¹⁸ and $I = 0$ for Cl⁻). Also, the $K_{\text{CaSO}_4}^0$ value is larger than the K_1^0 values of CdX₂. The K values were in the order $K_{\text{CaSO}_4}^0 > K_1^0 > K_2^0$. These facts suggest that the Coulombic force ($\propto |z_+z_-|$) is a dominant one in any interaction between Cd²⁺ and SO₄²⁻ or Cd²⁺ and X⁻. The same is partially true of the CaX₂ and CaSO₄ systems: $K_{\text{CaSO}_4}^0 = 150 \text{ mol}^{-1}\cdot\text{dm}^3$ and 1/0.0053 (see p 416 in ref 21) at 25 °C in water.⁷ The K_1^0 values of MPic⁺ are somewhat larger than those of MCl⁺. The relationship $K_1^0(\text{CdX}^+) > K_1^0(\text{CaX}^+)$ is found for a given X⁻ (see Table 1). Especially, the relationship of K_1^0 for X = Cl must reflect a difference

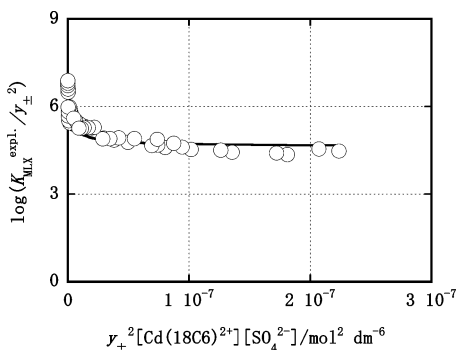


Figure 4. Plot of $\log(K_{MLX}^{exptl}/y_{\pm}^2)$ versus $y_{\pm}^2[CdL^{2+}][SO_4^{2-}]$ for $L = 18C6$. Solid line shows the curve fitted to eq 13a by the regression, where the emf data measured with the cells I and IK were used summarily for calculation of K_{MLX}^{exptl} .

between Cd^{2+} and Ca^{2+} in coordination ability to Cl^{-} , because both effective ionic radii are fairly close: 0.95 Å for Cd^{2+} and 1.00 Å for Ca^{2+} .²²

Ion-Pair Formation of CdL^{2+} with SO_4^{2-} . Figure 4 shows a plot of $\log(K_{MLX}^{exptl}/y_{\pm}^2)$ versus $y_{\pm}^2[CdL^{2+}][SO_4^{2-}]$ for $L = 18C6$. Similar to the curves in Figures 1 and 2 ($X = Pic$), a hyperbolic curve was observed. Analysis of the plot by the regression yielded the parameters, $K_{MLX}^0 = (4.38 \pm 0.68) \cdot 10^4 \text{ mol}^{-1} \cdot \text{dm}^3$ and $bm = (7.9 \pm 1.0) \cdot 10^{-4} \text{ mol} \cdot \text{dm}^{-3}$, with the curve of $R = 0.932$ at $n = 50$. Here, y_{\pm}^2 equals $y_{Cd(18C6)^{2+}} \cdot y_{SO_4^{2-}}$ and the $y_{Cd(18C6)^{2+}}$ values were calculated from the Davies equation,²³ because its ion size parameter was not available. Also, the $CdSO_4$ –B18C6 system yielded $K_{MLX}^0 = (1.83 \pm 0.51) \cdot 10^4 \text{ mol}^{-1} \cdot \text{dm}^3$ and $bm = (1.6 \pm 0.2) \cdot 10^{-3} \text{ mol} \cdot \text{dm}^{-3}$ at $R = 0.946$ and $n = 42$. In these two systems, there were no marked differences in K_{MLA}^{exptl} between the cells I and IK. This agreement demonstrates no appreciable effect of the complex formation of 18C6 or B18C6 with K^+ , leaking from a compartment of the reference electrode, on the K_{MLX}^{exptl} determination during the emf measurements of 35 to 40 min.

These $K_{CdLSO_4}^0$ values are much larger than the $K_{CdSO_4}^0$ one. Such facts have also been observed in the M^+X^- –18C6 and –B18C6 systems reported before.^{9,24} The K_{MLX}^0 value of the $CdSO_4$ –18C6 system is larger than that $(231 \text{ mol}^{-1} \cdot \text{dm}^3)^2$ of the $NaMnO_4$ –18C6 one by a factor of about 190. The sizes of Na^+ (ionic radius = 1.02 Å) and MnO_4^- (2.4 Å) are close to those of Cd^{2+} (0.95 Å) and SO_4^{2-} (2.3 Å), respectively.^{22,25} Hence, the difference between the two K_{MLX}^0 values should come from mainly the electric charge, $|z_+z_-|$, among these ions which constitute the corresponding ion-pairs. The same is essentially true of the $CdSO_4$ –B18C6 system: $K_{Cd(B18C6)SO_4}^0 > K_{Na(B18C6)MnO_4}^0 (= 1.6 \cdot 10^3 \text{ mol}^{-1} \cdot \text{dm}^3)$.²⁴

From the $K_{Cd(18C6)SO_4}^0$ value, the Bjerrum distance of closest approach (see pp 392–397 in ref 21) was calculated to be 1.8 Å, where it was assumed that $K_{CdLSO_4}^0$ was equivalent with Bjerrum's ion-pair formation constant.²⁴ This value is smaller than the sum (3.3 Å) in ionic radius between Cd^{2+} and SO_4^{2-} . From the same calculation, the distance of closest approach for $CdSO_4$ was estimated to be 4.4 Å. These findings suggest a direct interaction between Cd^{2+} held in the 18C6 ring and SO_4^{2-} . The same result was obtained for the $CdSO_4$ –B18C6 system (the distance of closest approach being 1.9 Å).

Literature Cited

- (1) Takeda, Y.; Yasui, A.; Morita, M.; Katsuta, S. Extraction of Sodium and Potassium Perchlorates with Benzo-18-crown-6 into Various

Organic Solvents. Quantitative Elucidation of Anion Effects on the Extraction-ability and -selectivity for Na^+ and K^+ . *Talanta* **2002**, *56*, 505–513.

- (2) Kudo, Y.; Usami, J.; Katsuta, S.; Takeda, Y. Solvent Extraction of Permanganates (Na , K) by 18-Crown-6 Ether from Water into 1,2-Dichloroethane: Elucidation of an Extraction Equilibrium Based on Component Equilibria. *Talanta* **2003**, *59*, 1213–1218.
- (3) Takeda, Y. Extraction of Alkali Metal Picrates with 18-Crown-6, Benzo-18-crown-6, and Dibenzo-18-crown-6 into Various Organic Solvents. Elucidation of Fundamental Equilibria Governing the Extraction-ability and -selectivity. *Bunseki Kagaku* **2002**, *51*, 515–525 (in Japanese).
- (4) Kudo, Y.; Usami, J.; Katsuta, S.; Takeda, Y. On the Difference between Ion-pair Formation Constants of Crown ether-complex Ions with Picrate Ion in Water Determined by Solvent Extraction and Potentiometry. *J. Mol. Liq.* **2006**, *123*, 29–37.
- (5) Vanderzee, C. E.; Dawson, H. J., Jr. The Stability Constants of Cadmium Chloride Complexes: Variation with Temperature and Ionic Strength. *J. Am. Chem. Soc.* **1953**, *75*, 5659–5663.
- (6) Harned, H. S.; Fitzgerald, M. E. The Thermodynamics of Cadmium Chloride in Aqueous Solution from Electromotive Force Measurements. *J. Am. Chem. Soc.* **1936**, *58*, 2624–2629.
- (7) Katayama, S. Conductimetric Determination of Ion-association Constants for Calcium, Cobalt, Zinc, and Cadmium Sulfates in Aqueous Solutions at Various Temperatures between 0 °C and 45 °C. *J. Solution Chem.* **1976**, *5*, 241–248.
- (8) Kudo, Y.; Usami, J.; Katsuta, S.; Takeda, Y. Solvent Extraction of Silver Picrate by 3*m*-Crown-*m* Ether ($m = 5, 6$) and Its Mono-benzo-derivative from Water into Benzene or Chloroform: Elucidation of an Extraction Equilibrium Using Component Equilibrium Constants. *Talanta* **2004**, *62*, 701–706.
- (9) Kudo, Y.; Wakasa, M.; Ito, T.; Usami, J.; Katsuta, S.; Takeda, Y. Determination of Ion-pair Formation Constants of Univalent Metal-crown ether Complex Ions with Anions in Water Using Ion-selective Electrodes: Application of Modified Determination Methods to Several Salts. *Anal. Bioanal. Chem.* **2005**, *381*, 456–463.
- (10) Takeda, Y.; Mochizuki, Y.; Tanaka, M.; Kudo, Y.; Katsuta, S. Conductance Study of 1:1 19-Crown-6 Complexes with Various Mono- and Bivalent Metal Ions in Water. *J. Incl. Phenom. Macrocycl. Chem.* **1999**, *33*, 217–231.
- (11) Katsuta, S.; Tsuchiya, F.; Takeda, Y. Equilibrium Studies on Complexation in Water and Solvent Extraction of Zinc(II) and Cadmium(II) with Benzo-18-crown-6. *Talanta* **2000**, *51*, 637–644.
- (12) Kielland, Y. Individual Activity Coefficients of Ions in Aqueous Solutions. *J. Am. Chem. Soc.* **1937**, *59*, 1675–1678.
- (13) Kudo, Y.; Fujihara, R.; Katsuta, S.; Takeda, Y. Solvent Extraction of Sodium Perrhenate by 3*m*-Crown-*m* Ethers ($m = 5, 6$) and Their Mono-benzo-derivatives into 1,2-Dichloroethane: Elucidation of an Overall Extraction Equilibrium Based on Component Equilibria Containing an Ion-pair Formation in Water. *Talanta* **2007**, *71*, 656–661.
- (14) Davies, C. W. The Extent of Dissociation of Salts in Water. Part VIII. An Equation for the Mean Ionic Activity Coefficient of an Electrolyte in Water, and a Revision of the Dissociation Constants of Some Sulphates. *J. Chem. Soc.* **1938**, 2093–2098.
- (15) Rudolph, W.; Irmer, G. Raman and Infrared Spectroscopic Investigation of Contact Ion Pair Formation in Aqueous Cadmium Sulfate Solutions. *J. Solution Chem.* **1994**, *23*, 663–684.
- (16) Rudolph, W.; Irmer, G.; Hefter, G. T. Raman and Infrared Spectroscopic Investigation of Speciation in $MgSO_4$ (aq). *Phys. Chem. Chem. Phys.* **2003**, *5*, 5253–5261.
- (17) King, E. L. Thermodynamic Data on the Cadmium Chloride Complexes Determined from the Solubility of Cadmium Ferricyanide. *J. Am. Chem. Soc.* **1949**, *71*, 319–322.
- (18) Gerding, P. Thermochemical Studies on Metal Complexes I. Free Energy, Enthalpy, and Entropy Changes for Stepwise Formation of Cadmium(II) Halide Complexes in Aqueous Solution at 25 °C. *Acta Chim. Scand.* **1966**, *20*, 79–94.
- (19) DeFord, D. D.; Hume, D. N. The Determination of Consecutive Formation Constants of Complex Ions from Polarographic Data. *J. Am. Chem. Soc.* **1951**, *73*, 5321–5322.
- (20) Hume, D. N.; DeFord, D. D.; Cave, G. C. B. A Polarographic Study of the Cadmium Thiocyanate Complexes. *J. Am. Chem. Soc.* **1951**, *73*, 5323–5325.
- (21) Robinson, R. A.; Stokes, R. H. *Electrolyte Solutions*, 2nd revised ed.; Dover: New York, 1959; Appendix 2.1.
- (22) Shannon, R. D. Revised Effective Ionic Radii and Systematic Studies of Interatomic Distances in Halides and Chalcogenides. *Acta Crystallogr.* **1976**, *A32*, 751–767.

- (23) de Levie, R. *Aqueous Acid–Base Equilibria and Titration*; Compton, R. G., Ed.; Oxford Chemistry Primers 80; Oxford University Press: New York, 1999; p 62.
- (24) Kudo, Y.; Fujihara, R.; Ohtake, T.; Wakasa, M.; Katsuta, S.; Takeda, Y. Ion-pair Formation of 3*m*-Crown-*m* Ether ($m = 5, 6$) and Its Mono-benzo-derivative Complex Ions with Several Pairing Anions in Water. *J. Chem. Eng. Data* **2006**, *51*, 604–608.
- (25) Marcus, Y. *Ion Properties*; Dekker: New York, 1997; Chapter 3, pp 43–62 (see Table 3).

Received for review March 15, 2007. Accepted June 30, 2007.

JE700135J